

## WETTING BETWEEN CARBON AND CRYOLITIC MELTS. PART II: EFFECT OF BATH PROPERTIES AND POLARISATION

Asbjørn Solheim<sup>1</sup>, Henrik Gudbrandsen<sup>1</sup>, Ana Maria Martinez<sup>1</sup>, Kristian Etienne Einarsrud<sup>2</sup>, and Ingo Eick<sup>3</sup>

<sup>1</sup> SINTEF Materials and Chemistry, Trondheim, Norway, <sup>2</sup> HiST, Trondheim, Norway, <sup>3</sup> Hydro Aluminium, Neuss, Germany

Key words: Wetting; Carbon; Cryolite; Alumina; Polarisation

### Abstract

An apparatus for determination of wetting angles, based on the immersion-emersion technique and adapted for use at high temperature, was used for measuring the wetting between cryolitic melts and samples consisting of standard anode carbon. Anodic polarisation of the sample and the alumina concentration were the more important factors. Polarisation strongly improved the wetting if the melt was low in alumina, and the effect persisted for a while after the current was turned off. Increasing the alumina concentration to near saturation brought about a dramatic change from non-wetting to good wetting. The advancing angle of wetting was normally larger than the receding angle, while the opposite was observed in some experiments with aqueous solutions of ethanol and sodium fluoride. The latter effect has interesting consequences for the motion of gas bubbles, and the results also demonstrate that it is necessary to be careful in the selection of liquids and materials for physical modelling of aluminium cells.

### Introduction

Detailed understanding of interfaces and interfacial processes is of vital importance for the aluminium industry, since nearly all important processes in aluminium cells take place at interfaces. Some examples are the electrode reactions, formation of sideedge, and cathode wear. Many important properties depend on wetting between bath or metal and carbon materials, as outlined in Part I of the present work<sup>[1]</sup>.

Some work concerning wetting between cryolitic melts and carbon materials has been reported in the literature. The work is discussed in "Aluminium Electrolysis"<sup>[2, 3]</sup>. The trends can be summarised as follows,

- For melt compositions close to industrial bath, the angle of wetting at amorphous carbon as well as at graphite is about 130°.
- The angle of wetting decreases with increasing temperature. The temperature dependence is stronger with amorphous carbon than with graphite.
- The angle of wetting increases with increasing contents of AlF<sub>3</sub> in the bath, and it decreases with increasing alumina concentration. The effect of other bath additives (except NaCl) appears to be somewhat disputed<sup>[2, 3]</sup>.
- For melts with NaF/AlF<sub>3</sub> ratios higher than 3, the wetting angle decreases with increasing time of contact between the melt and carbon.

Experimental investigation of the influence of polarisation is scarce. Qiu *et al.* (cited in "Aluminium Electrolysis"<sup>[3]</sup>) found that cathodic polarisation of graphite in contact with a cryolitic melt

decreased the wetting angle considerably, while there was a minimum at current densities about 1-2 Acm<sup>-2</sup> during anodic polarisation. With a non-polarised sample or with cathodic polarisation the wetting angle increased with increasing contact time, while it decreased with time during anodic polarisation.

The present paper reports the first measurements made with cryolite and industrial anode carbon, as well as some results obtained with aqueous solutions of ethanol and sodium chloride and a ceramic.

### Experimental

#### Bath and Sample

The samples used in cryolitic melts were made from industrial anode carbon and shaped as an inverted cup with inner and outer diameters of 35 and 40 mm, respectively. The sample was fastened to a 250 mm long steel rod (6 mm dia.) suspended in a platinum wire to ensure that the lower surface of the sample was horizontal. Current cables were attached to the steel rod to enable measurements during polarisation, and an extra weight was attached to the top of the sample to ensure that the bottom of the sample was horizontal.

The bath was taken from a shut-down industrial cell. The analysis showed 12.0 wt% excess AlF<sub>2</sub>, 4.6 wt% CaF<sub>2</sub>, and 1.0 wt% Al<sub>2</sub>O<sub>3</sub>, corresponding to a NaF/AlF<sub>3</sub> molar ratio of 2.2. Experiments were made with this bath and the same composition with added alumina (11.2 wt% AlF<sub>3</sub>, 4.3 wt% CaF<sub>2</sub>, and 8.0 wt% Al<sub>2</sub>O<sub>3</sub>). The surface tension of these compositions as a function of the temperature is shown in Figure 1, based on the equation by Danek *et al.*<sup>[4]</sup>.

The calculated weight due to the interfacial forces is shown as a function of the wetting angle in Figure 2 (see Part I of the present work<sup>[1]</sup>). Negative values correspond to de-wetting; *i.e.*, the surface forces work in the opposite direction of the gravity.

Some measurements were also made with water/ethanol mixtures and with solutions of NaCl in water. In these measurements a plate-shaped porous ceramic material was used; this was the same material as used for creating bubbles in a physical model<sup>[5]</sup>.

#### Measuring Sequences

In the "hot" measurements three types of sequences were used,

- A. Start with the sample about 5 mm above the melt and immerse the sample by 40 mm (*i.e.*, lift the crucible, see Part I<sup>[1]</sup>) at a rate of 0.2 mm/s. Return to the start position at 0.2 mm/s.
- B. Immerse the sample to position 40 mm at 0.2 mm/s. Stop for 10 min. Move to position 35 mm at 0.2 mm/s and wait for 10 min. Return to the start position at 0.2 mm/s.

- C. Immerse the sample to position 40 mm at 0.2 mm/s. Stop for 10 min. Apply anodic current (50 A) for 10 s. Return to the start position at 0.2 mm/s.

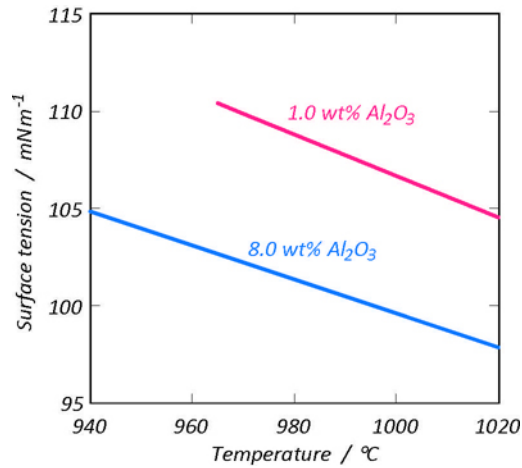


Figure 1. Surface tension for the bath compositions (see text) as a function of the temperature, according to the equation by Danek *et al.* [3].

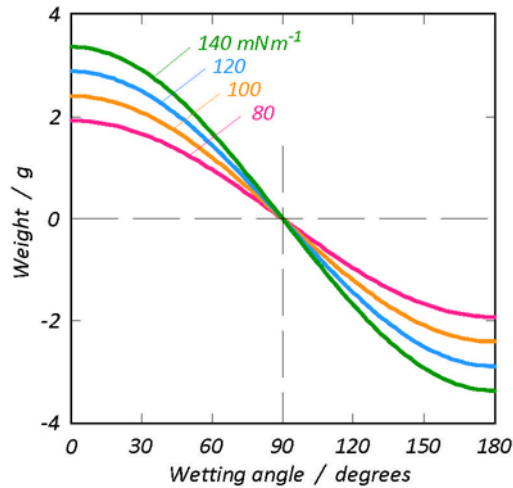


Figure 2. Weight due to surface forces as a function of the wetting angle at different values of the surface tension (the length of the meniscus is 235.6 mm).

### Results with Carbon and Cryolitic Melts

#### Low Alumina Concentration

When the sample was not polarised, the measured weight of the meniscus (the difference between the recorded weight ( $m_m$ ) and the theoretical weight in absence of surface forces ( $m_t$ )) was constant, during immersion as well as during emersion. The samples were strongly de-wetted, as is manifested by a force acting upwards (negative weight difference, as shown in Figure 3 for a recording with type A measuring sequence). Part of the "noise" in the curves reflects the reality; in testing with water it could be observed that the meniscus was jagged and showed stepwise motion, instead of sliding smoothly along the sample.

The results with type B measuring sequence usually produced curves similar to the one shown in Figure 3. The intention with the 10 min breaks was to study the relaxation of the advancing or receding wetting angle to the equilibrium angle. Two relaxation curves are shown in Figure 4. As can be observed, very little happened when the break was made during emersion (curve II in Figure 4). When stopping during immersion (curve I), one would expect that the weight difference should decrease, provided that the equilibrium wetting angle is between the advancing and the receding angles. The increasing difference shown in Figure 4 may reflect the above mentioned observation that the wetting angle depends on the contact time.

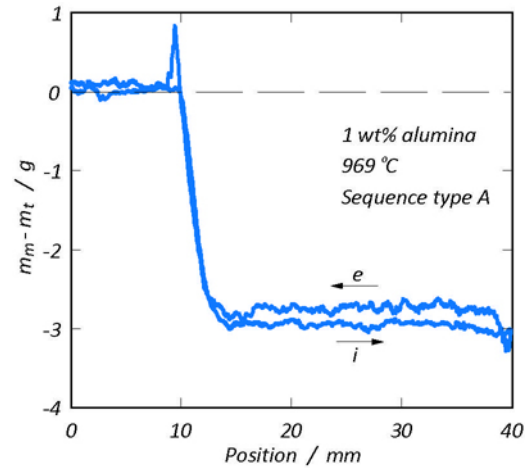


Figure 3. Difference between the recorded weight ( $m_m$ ) and the theoretical weight ( $m_t$ ) as a function of the position for a non-polarised sample. i – immersion (advancing wetting angle), e – emersion (receding wetting angle).

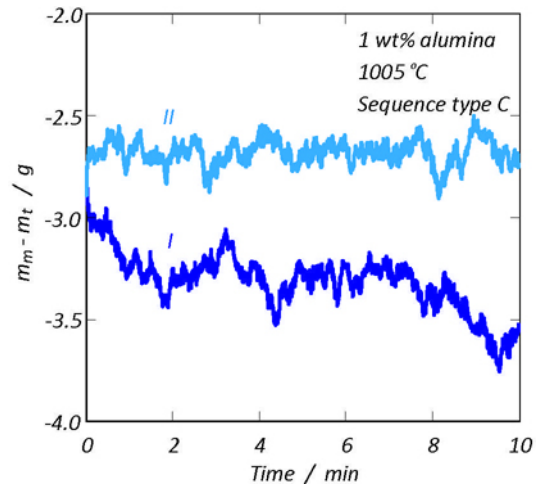


Figure 4. Difference between the recorded weight ( $m_m$ ) and the theoretical weight ( $m_t$ ) during break for relaxation. I – stop at position 40 mm (from immersion towards equilibrium), II – stop at 35 mm (from emersion towards equilibrium).

When the samples were polarised after being fully immersed, the wetting improved (sequence C). The wetting was permanently improved after the current had been switched off after the second polarisation. The improvement of the first polarisation relaxed until the sample was emerged from the bath. Two different sets of data are shown in Figure 5. The difference between the curves might be caused by the fact that the data recorded at 969 °C (black line) represents the first polarisation, while the data at 987 °C (blue line) represents the second polarisation.

After the sample had been subjected to polarisation, it had apparently changed permanently, which must be due to adsorbed substances at the sample surface. The curve in Figure 6 was obtained without polarisation immediately after the curve recorded at 987 °C shown in Figure 5. It is noteworthy that only the wetting during emersion was affected; the measured weight during immersion was always the same.

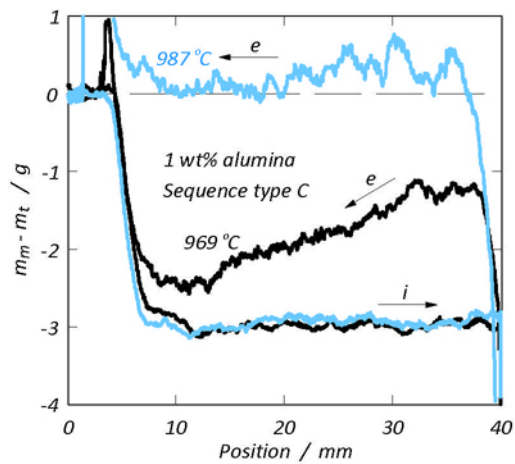


Figure 5. Difference between the recorded weight ( $m_m$ ) and the theoretical weight ( $m_t$ ) as a function of the position (two different experiments). The samples were polarised at 50 A for 10 s at position 40 mm. Black line – first polarisation, blue line – second polarisation.

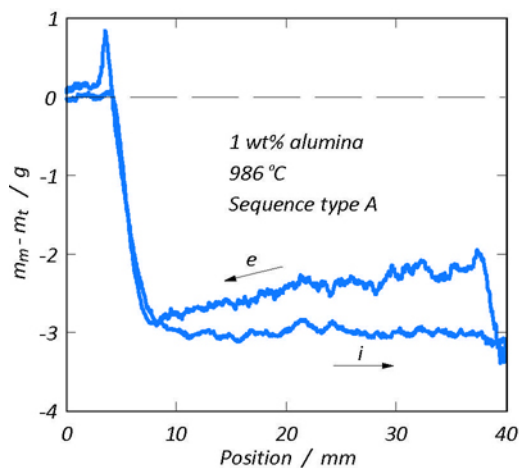


Figure 6. Difference between the recorded weight ( $m_m$ ) and the theoretical weight ( $m_t$ ) as a function of the position.

### High Alumina Concentration

The wetting conditions changed dramatically when the alumina concentration was increased to 8 wt%. Apparently, the conditions changed from completely de-wetting to completely wetting. Polarisation did not affect the wetting so much, since the sample already was well wetted. It appeared that the upper part of the sample had lower angle of wetting (smaller weight difference at high crucible position) and there was generally much more scatter and variation in the data than in the data obtained in a melt low in alumina. The change in the wetting conditions also influenced the weight course during the time contact was made, as shown in Figure 7. The 5 g higher weight with 8 wt% alumina can for a large part be ascribed to bath penetrating into the sample, and there was probably also a film of bath present at the surface. After finishing the experiment solidified bath adhered strongly to the sample, which was not the case when using the low alumina bath.

Figure 8 shows two curves obtained with different temperatures and measuring sequences.

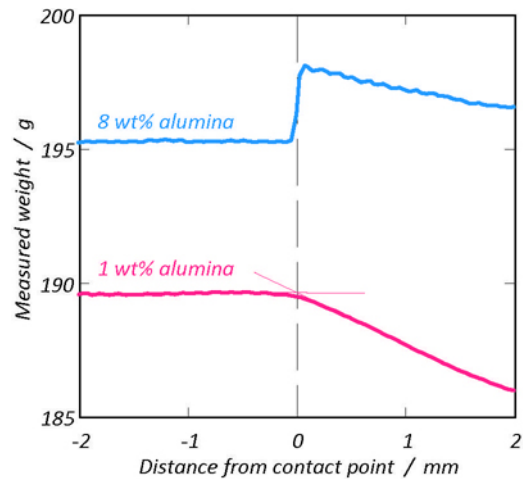


Figure 7. Recorded weight as a function of the position around the contact point.

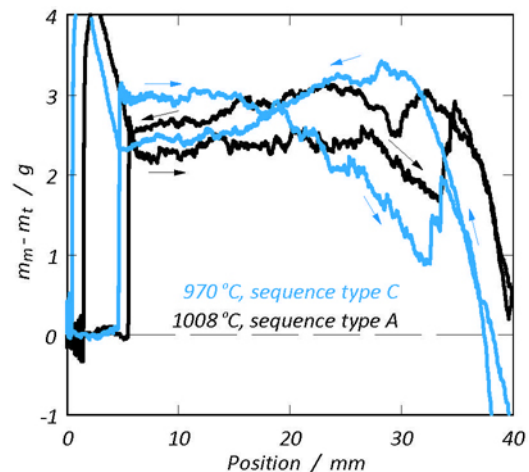


Figure 8. Difference between the recorded weight ( $m_m$ ) and the theoretical weight ( $m_t$ ) as a function of the position (two different experiments).

The relaxation courses during the 10 min stops are shown in Figure 9. As can be observed, the behaviour resembles the data obtained with 1 wt% alumina (Figure 4), but the weight levels are completely different.

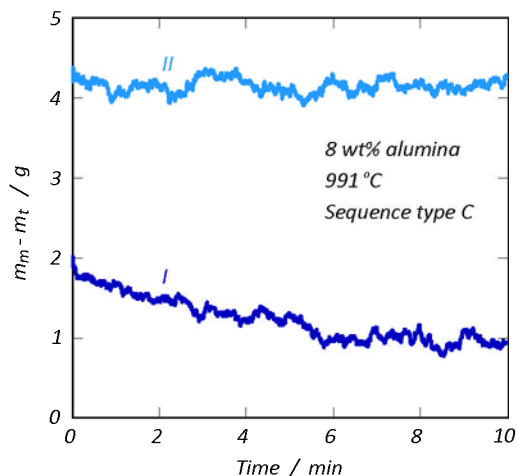


Figure 9. Difference between the recorded weight ( $m_m$ ) and the theoretical weight ( $m_t$ ) during stop for relaxation. I – stop at position 40 mm (from immersion towards equilibrium), II – stop at 35 mm (from emersion towards equilibrium).

### The Advancing Angle of Wetting

As was indicated above, the weight difference during immersion (advancing wetting angle) showed little variation. This means that the advancing wetting angle (which will be at the trailing part of a bubble moving along the anode) is almost independent of the conditions, except the alumina concentration. The recorded weight changes during immersion are shown as a function of the temperature in Figure 10. The data are derived by taking the average of all recordings in the position range 15-35 mm for 1 wt% alumina and 10-20 mm for 8 % alumina; the latter represents the almost horizontal region at the lower part of the sample. The figure contains data from all types of measuring cycles.

The results in Figure 10 were somewhat surprising. There is a striking difference that must be attributed to the alumina concentration, but there is very little variation with temperature. The surface tension decreases with increasing temperature, and it has also been reported in the literature that the wetting angle decreases with increasing temperature. Therefore, it was expected to see a difference at least in the set of data obtained with low alumina concentration.

### Results with Aqueous Solutions and Ceramic

In order to support the development of a model for bubble driven flow [6], water model experiments were carried out. Anodic gas evolution was simulated by passing compressed air through a ceramic plate fastened to the bottom of a 10 x 10 cm PMMA box, and the gas-evolving surface was recorded by video from below. The results are described by Simonsen *et al.* [5]. Figure 11 shows a picture taken from their paper.

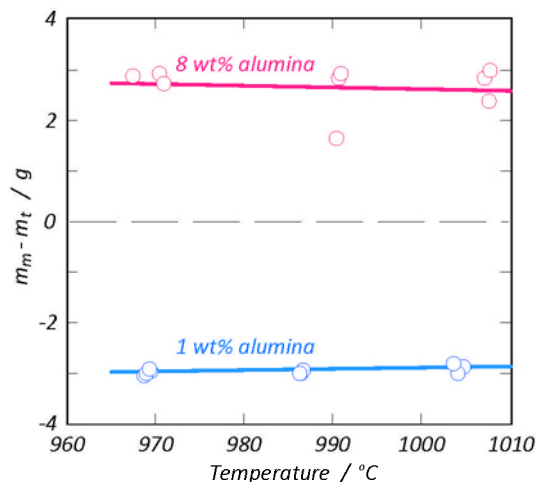


Figure 10. Difference between the recorded weight ( $m_m$ ) and the theoretical weight ( $m_t$ ) during immersion (advancing angle of wetting) as a function of the temperature. The figure shows all results, regardless of the measuring cycle. Symbols – experimental results, lines – trend lines.

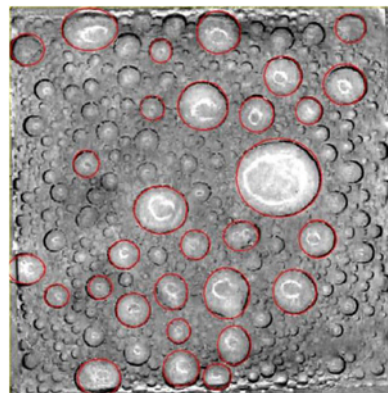


Figure 11. Gas bubbles formed by passing compressed air through a ceramic plate. The largest bubbles are marked in red. The picture was taken from the work by Simonsen *et al.* [5].

In the water model, striking differences in the bubble behaviour were observed, depending on the liquid used. It was therefore decided to carry out measurements in the wetting apparatus using the same solid and liquids as used in the model.

A piece of the ceramic filter material used in the model was cut into a rectangular plate with dimensions 49.6 x 40 x 2.0 mm, which was suspended from two wires to keep it horizontal. It was necessary to introduce a small extra correction factor to account for the liquid penetrating into the porous ceramic, which will not be further commented here.

Measurements were carried out at room temperature using aqueous solutions of ethanol and sodium chloride in water. It turned out that at high concentrations of sodium chloride or

ethanol, the advancing wetting angle became smaller than the receding angle. This was particularly pronounced with the ethanol solutions. Figure 12 shows a recording with 15 wt% ethanol, while the difference between the weights recorded during emersion ( $m_{rec}$ ) and during immersion ( $m_{adv}$ ) is shown in Figure 13. As can be observed, the receding angle became larger than the advancing angle when the concentration exceeded 15 wt% sodium chloride or 5 wt% ethanol.

As mentioned in Part I of the present work [1], this type of odd behaviour was also observed with the combination of quartz and water.

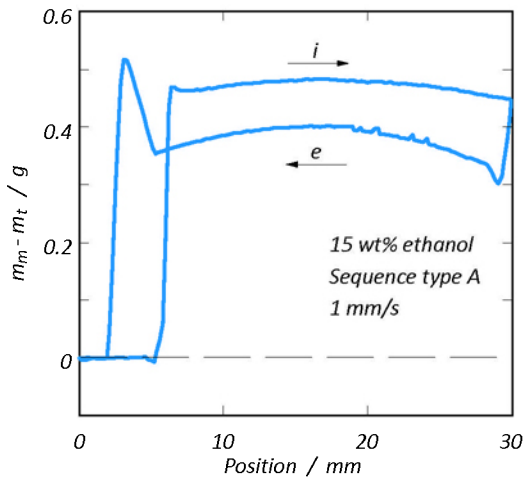


Figure 12. Difference between the recorded weight ( $m_m$ ) and the theoretical weight ( $m_t$ ) as a function of the position for an experiment with a ceramic plate in a solution with 15 wt% ethanol. The beaker was moved at a rate of 1 mm/s.

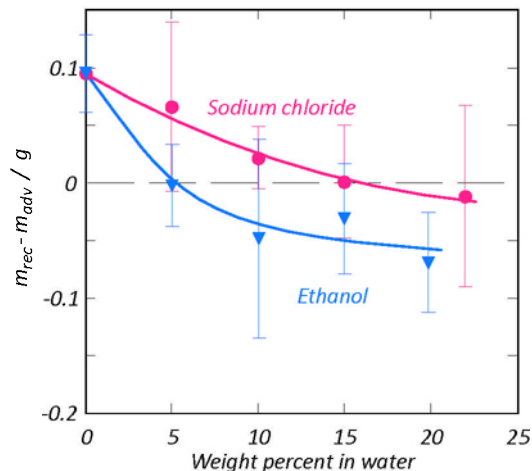


Figure 13. The difference between the weight recorded during emersion and the weight recorded during immersion for the combination of a ceramic plate and different aqueous solutions. Each data point represents measurements where the beaker was translated at 0.05, 0.2, and 1.0 mm/s.

## Discussion

### Surface Tension of Cryolitic Melts

The measured weights due to surface forces are higher in the present work than what is theoretically possible. The surface tension is in the range 100-110 mNm<sup>-1</sup> as shown in Figure 1, and the maximum possible weight (with 180 ° wetting angle) is about 2.5 g, while the recorded weights could be more than 3 g. A possible source of error is that if the sample is suspended at an angle, the buoyancy correction would easily become erroneous. It can be estimated, however, that it takes a lop-sidedness of more than 1.5 mm at the bottom of the sample to cause an error of 0.5 g, which we regard impossible. This would also have been discovered from the measured weight at the time the sample touches the melt surface. The slightly gradual progress in the weight change shown in Figure 7 (1 wt% alumina) is probably due to repulsive forces between the sample and the melt.

Since the data presented here indicate a somewhat larger force than what can be explained from the surface tension data, the results are presented as weights rather than as wetting angles. In further work it will be prioritised to come up with solid explanations for the apparently too high surface force.

### Effect of Alumina

Wetting between carbon and cryolitic melts appears to be extremely complicated, depending on polarisation and time as well as the properties of the melt and the carbon material. The effect of the alumina concentration was much higher than what could be anticipated from literature data, while the temperature influence was smaller. The natural next step is to carry out measurements with several different alumina concentrations. If the present data are correct, this strongly supports the hypothesis that the abrupt voltage decrease following the anode effect is due to de-wetting and the formation of a gas film underneath the anode as described by Vogt [7].

### Advancing and Receding Wetting Angles

The advancing wetting angle is normally higher than the receding angle. This is the reason why a raindrop can reside on a vertical window pane (the gravity is balanced by the surface forces acting in the direction parallel to the solid surface). In some cases in the present work, it was observed that the advancing wetting angle was smaller than the receding angle. This kind of unusual wetting behaviour can probably be explained by adsorption and desorption close to the meniscus. Evaporation from the meniscus may also be involved; the latter effect explains the formation of a film inside a cognac glass leading to cognac droplets at the top of the film.

The phenomenon opens up the possibility of quite bizarre behaviour (such as droplets creeping upwards along a slanting surface). It can be deduced that a bubble will start moving in an arbitrary direction, independent of the gravity, depending on the direction of the first impulse. Such self-propelled motion has been described for bubbles on a solid surface when an electric field was applied; citation [8]. *The initial direction of the motion is unpredictable, but once started, it persists until the droplet reaches the end of the electrodes or the voltage is turned off.*

Bubble motion in the opposite direction of gravity was, in fact, observed in the water model by Simonsen *et al.* [5]. While this might be due to smaller advancing than receding wetting angle, it

is also possible that the behaviour can be ascribed to fluid flow, which in the water model consisted of a double vortex pair in the ACD. To the authors' knowledge, self-propelling bubbles on anode surfaces has not been reported in the literature.

As the abnormal contact angle behaviour was not observed in the cryolite-carbon system; pure water appears to be the best candidate for water model experiments, based upon good agreement in relevant dimensionless numbers and wetting properties, as indicated in the current work. However, as indicated by Simonsen *et al.* [5], saline solutions appear to more easily promote a self-organized state in the bubble flow, despite the abnormal contact angle pair.

The level of wetting in itself is probably also important. In water models where the anode is well wetted, the bubbles are moving quite fast on a water film which is limiting coalescence. In industrial cells where the anode is less wetted by the liquid (at least if the melt is not saturated in alumina) the bubbles may move more slowly and with more coalescence.

The above statements clearly illustrate the complexity of the phenomena occurring close to the anode surface.

#### Acknowledgement

The present work was supported by two projects financed by Hydro Aluminium and the Research Council of Norway, "HAL Ultra Performance Aluminium Cell" (HAL UP) and "Gas and Alumina Distribution and Transport" (GADT). Permission to publish the results is gratefully acknowledged.

#### References

1. A. M. Martinez, O. Paulsen, A. Solheim, H. Gudbrandsen, and I. Eick, "Wetting between Carbon and Cryolitic Melts. Part I: Theory and Equipment", *Light Metals 2015* (this volume).
2. K. Grjotheim, C. Krohn, M. Malinovsky, K. Matiasovsky, and J. Thonstad, *Aluminium Electrolysis*, 2<sup>nd</sup> Edition, Aluminium-Verlag, Düsseldorf, 1982.
3. J. Thonstad, P. Fellner, G.M. Haarberg, J. Hives, H. Kvande, and Å. Sterten, *Aluminium Electrolysis*, 3<sup>rd</sup> Edition, Aluminium-Verlag, Düsseldorf, 2001.
4. V. Danek, O. Patarak, and T. Østvold, "Surface Tension of Cryolite-Based Melts", *Can. Met. Quart.*, **34** (2) (1995), pp. 129/33.
5. A. Simonsen, K.E. Einarsrud, I. Eick, "The Impact of Bubble-Bubble Interactions on Anodic Gas Release": A Water Model Analysis, *Light Metals 2015* (this volume).
6. K.E. Einarsrud, I. Eick, P. Witt, A. Solheim, and Y. Feng, "Impact of Variable Bath Chemistry and Wetting on Gas Bubble Flow in Aluminium Electrolysis Cells", *Light Metals 2015* (this volume).
7. H. Vogt, "Contribution to the Interpretation of the Anode Effect", *Electrochimica Acta*, **42** (17) (1997), pp. 2691/705.
8. M. Gunji and M. Washizu, "Self-propulsion of a Water Droplet in an Electric Field", *J. Phys. D: Appl. Phys.* **38** (2005), pp. 2417/23.